SMARTUQ®

Quantify Every Uncertainty™

SmartUQ Engineering Analytics Light-Weighting Application

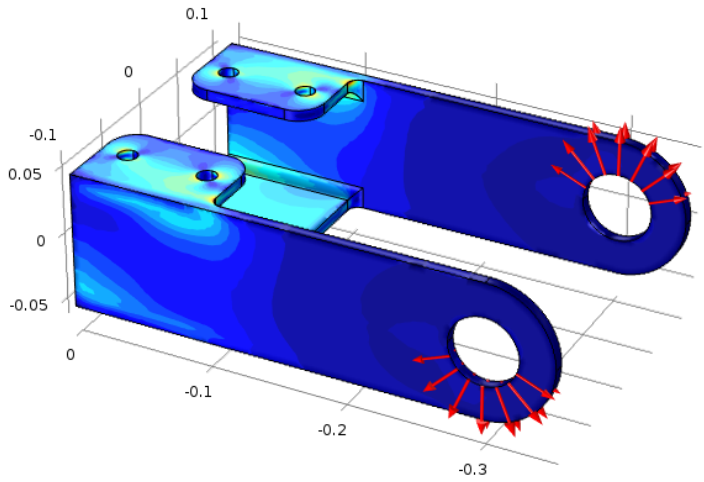

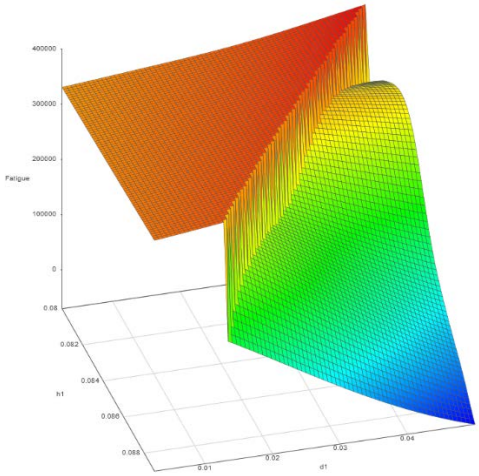

with COMSOL FEA Bracket Example

SmartUQ Engineering Analytics Light-Weighting Application with COMSOL FEA Bracket Example

Abstract

For decades, light-weighting has been a major area of research and concern in the automotive and aerospace industries. Industry leaders are adopting new software tools and investing ever greater engineering resources in adapting and optimizing their designs to be as lightweight and durable as possible. This paper documents an application of SmartUQ's engineering analytics capabilities to a mounting bracket subject to fatigue testing. This demonstration will detail the process of parameterizing a design, generating training data, and developing and improving sets of surrogate models. SmartUQ analytics tools are then used to optimize the design, zero in on key design parameters to inform future design decisions, and quantify the uncertainties around the optimal bracket configuration. A light weight design for the bracket is developed and shown to be robust to uncertainty. The geometry and FEA setup were based on COMSOL's application library bracket example.

Introduction

Background

The challenges associated with light-weighting are numerous and difficult to overcome. Light-weighting often results in elaborate geometries with large numbers of relevant inputs and very complex responses. This complexity makes it difficult to anticipate responses and the large number of inputs makes direct exploration of the design space infeasible. Finally, the constraints and goals of optimization are often conflicting. In this example, for instance, the reduction in mass comes at a cost of reduced fatigue life and increased displacement in parts of the bracket. Balancing these goals is difficult and most problems require advanced analytical tools to appropriately handle these challenges.

Overview

The geometry and FEA setup were based on COMSOL's application library bracket example with SmartUQ's partnership license. Parameterized slots cut into the bracket act as the mechanism by which weight optimization is performed on the bracket. The multiple failure modes evident in the simulations force the use of a discontinuous surrogate model to explore the design space. Adaptive design techniques allow the targeting of poorly defined failure modes to efficiently increase the accuracy of the surrogate model with as few simulations as possible. Sensitivity analysis is used to locate key input variables to inform future design decisions and constrained, multivariate optimization zeros in on an optimal bracket configuration. Uncertainty propagation is then performed on the optimal point to assess the robustness of the design to various geometric and material uncertainties. Finally, statistical calibration is used to correct for bias in the simulation results against a set of experimental test points.

Setup of the Simulation and Design of Experiment

The Bracket

A fatigue study performed on a steel bracket was chosen as the baseline model for this demonstration. As **Figure 1** illustrates, distributed loads were applied to the upper surface of one bolt hole and the lower surface of another to create a twisting motion. A single load-unload cycle was simulated to find the maximum Von Mises Stress, which was then applied to an S-n curve to determine the fatigue life of the design.

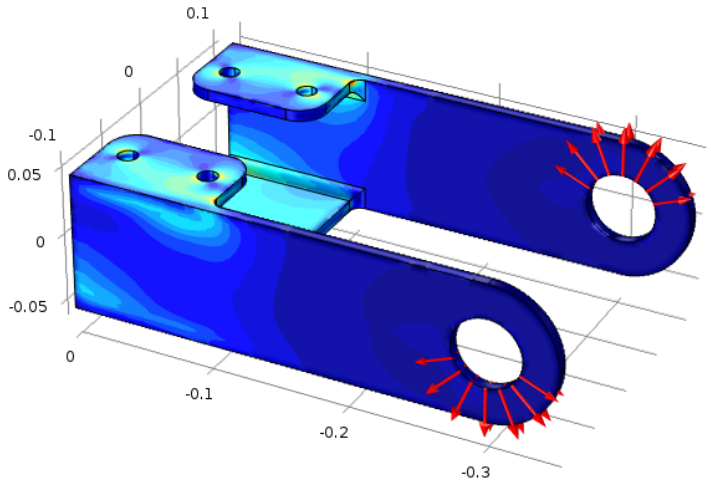

Figure 1: The stress contour of the original bracket design overlaid with the load distribution.

A few important metrics were measured from the original bracket design, as shown in **Table 1**. These metrics are the basis by which the performance of the optimized design will be assessed.

	Original Design
Mass (kg)	6.03
Maximum Displacement (mm)	2.28
Fatigue Life (N)	460000

Table 1: Design metrics for the original bracket design.

Alterations for Light-weighting Application

The bracket has a number of low stress areas along the sides and the bottom of the bracket that can be exploited for light-weighting purposes. **Figure 2** shows three parameterized slots that were cut into the bracket. The aim of this study will be to reduce the mass of the bracket as much as possible while maintaining an acceptable fatigue life and maximum displacement.

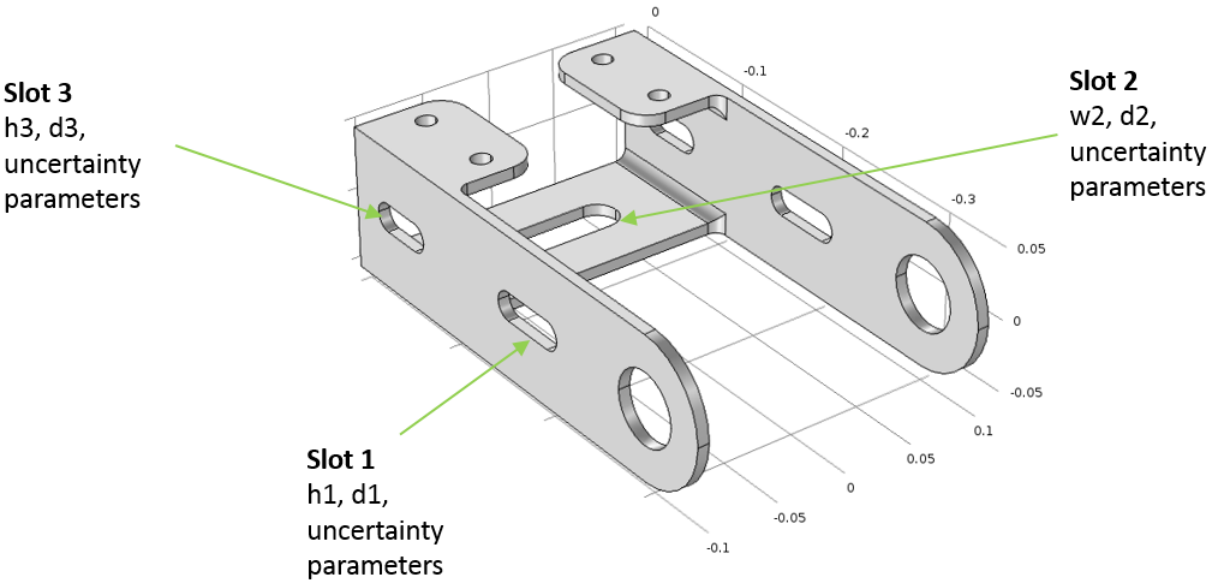

Figure 2: Bracket design with the integration of parameterized slots.

Each slot was assigned two geometric parameters describing its shape and size and two uncertainty parameters corresponding to machining tolerances. The uncertainty parameters, along with others that describe uncertainty in the material properties and general test conditions, will be described further in the portion of the report concerning uncertainty quantification. With the slots parameterized, a Design of Experiment (DOE) can be performed to begin the process of data generation.

Design of Experiment

The first step in the DOE process is coming up with a set of reasonable bounds for the input variables (in this case the geometric and uncertainty parameters). For now, only the geometric parameters will be discussed. Each geometric parameter is given a set of bounds such that the slots would not become so large they interfered with other features or extended through surfaces but not so small that were razor thin or pin sized defects. The geometric constraints are summarized in **Table 2**.

Parameters	Lower Bound	Upper Bound
h1	0.0025	0.09
d1	0.0025	0.05
h3	0.0025	0.04
d3	0.0025	0.05
w2	0.0025	0.08
d2	0.0025	0.08

Table 2: Design space constraints for geometric input parameters.

With the constraints set, it is possible to create the DOE. SmartUQ offers a wide range of advanced DOEs, each suited for different tasks. For this initial portion of the design, a Sliced Design is used. The Sliced

Design has the advantage of creating sets or slices of design points where each slice is an individually optimal Latin Hypercube Design (LHD). The slices can be combined in any number to form a larger optimal LHD. In this way, it is possible to load in design points incrementally until an emulator is trained to a desired level of accuracy. This is useful for computationally expensive tests where an unknown number of points are needed to train an emulator. **Figure 3** provides an example of the Sliced Design for visualization purposes.

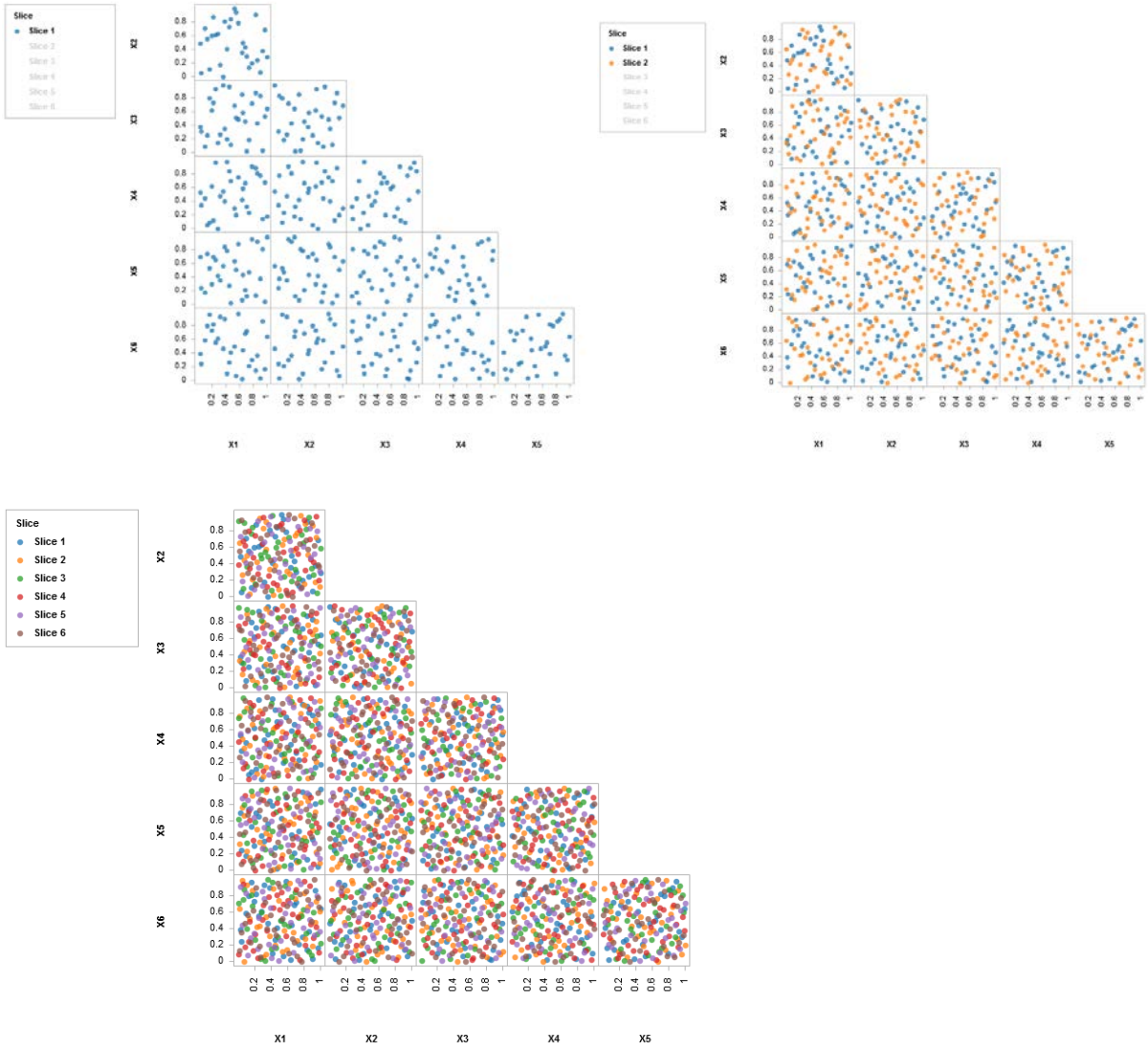

Figure 3: Implementation of a Sliced Design for a 6-dimensional input space.

As the figure illustrates, bringing in slices incrementally gives the design space increasing resolution with each iteration. For simple problems, a lower resolution design space, as pictured in the upper left corner of **Figure 3**, may be adequate. For more complex problems, a higher resolution design space, such as in the lower half of **Figure 3**, may be necessary.

The DOE for this problem contains twelve input parameters, six describing the geometric constraints and six describing uncertainties corresponding to machining tolerances and variation in the material properties and testing conditions that will be discussed further in the uncertainty quantification section.

Surrogate Modeling Process and Results

Generation of Training Data and Multivariate Emulation

After the DOE is created, training data is generated. Slices of 200 design points are run through COMSOL incrementally. The results from each slice, with their corresponding inputs, are then fed into SmartUQ to fit increasingly accurate emulators. A total of seven slices are used to train emulators. **Figure 4** shows a graphic illustrating a design surface and a scatter plot showing the cross-validation accuracy of the final emulator.

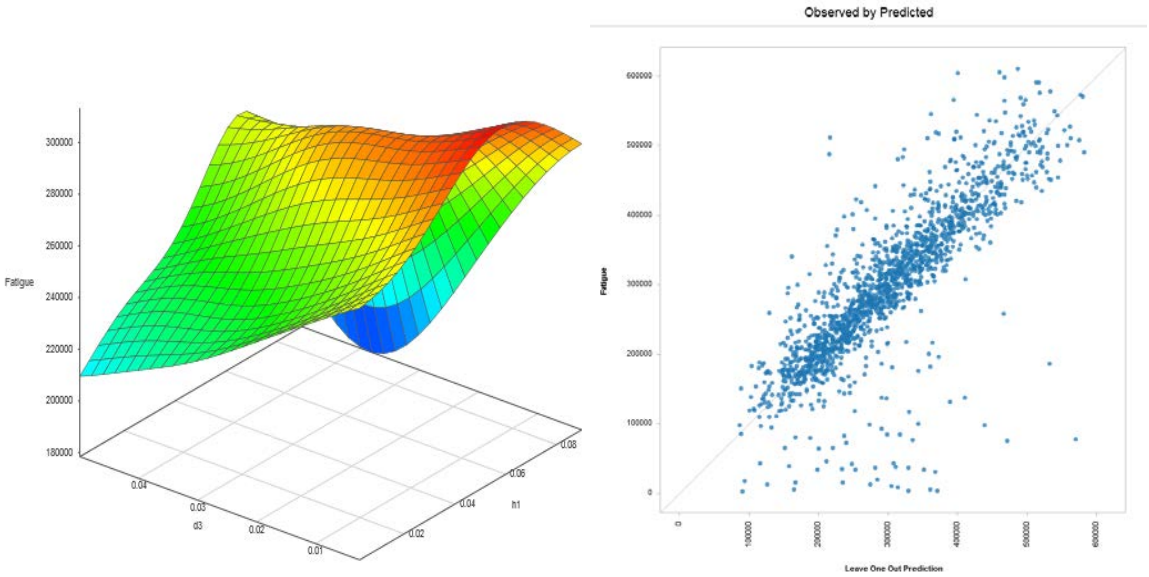

Figure 4: Emulator design surface plot (left) and fatigue training data vs Leave One Out Prediction (right).

As the right plot in **Figure 4** indicates, the agreement between the multivariate Emulator and training points is very poor. The number of design points generated in COMSOL should produce better results for a problem characterized by this level of complexity. This is a good indication that something more involved may be happening in the physics of this problem and that more investigation is needed.

Examination of COMSOL Results and Discussion of Failure Modes

Examining the results generated in COMSOL explains why the emulator is performing so poorly; as certain slots become too large or too thin, the location of fatigue failure shifts. In total, this bracket problem is characterized by six different failure modes. The multivariate emulator treats the training data set as a continuous function, which is adequate for most applications. However, the existence of several failure modes creates discontinuity in the failure patterns, and necessitates the implementation of an emulator can handle discontinuous functions to do further analysis. SmartUQ's Mixed Input Classification Emulator can handle this type of physical relationship, and will be implemented after the discussion of failure modes.

Figures 5-10 summarize the six different failure modes and their causes corresponding to particular configurations of the input parameters.

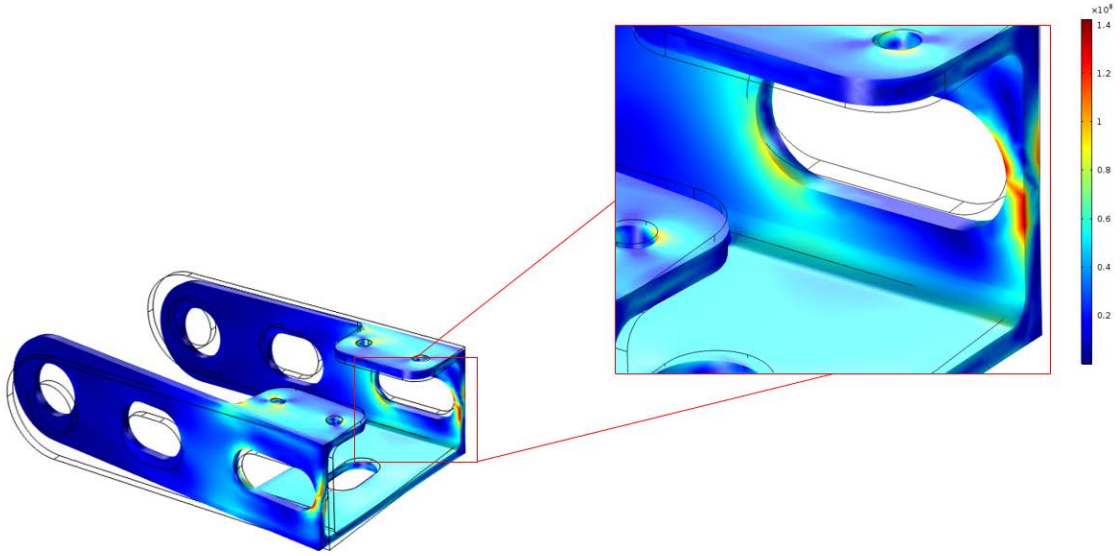

Figure 5: Failure mode A corresponds to an input set in which slot 3, characterized by the parameters h3 and d3, gets too large. This initiates fatigue failure on the back edge of the bracket.

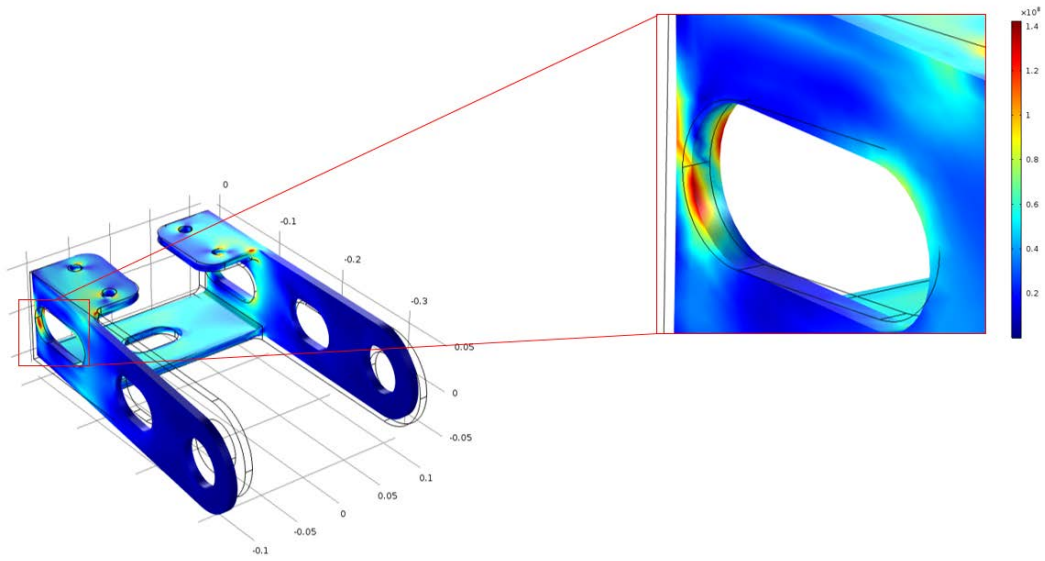

Figure 6: Failure mode B corresponds to a similar input set as mode A, but this particular input configuration causes fatigue failure to initiate on the inner edge of the bracket instead.

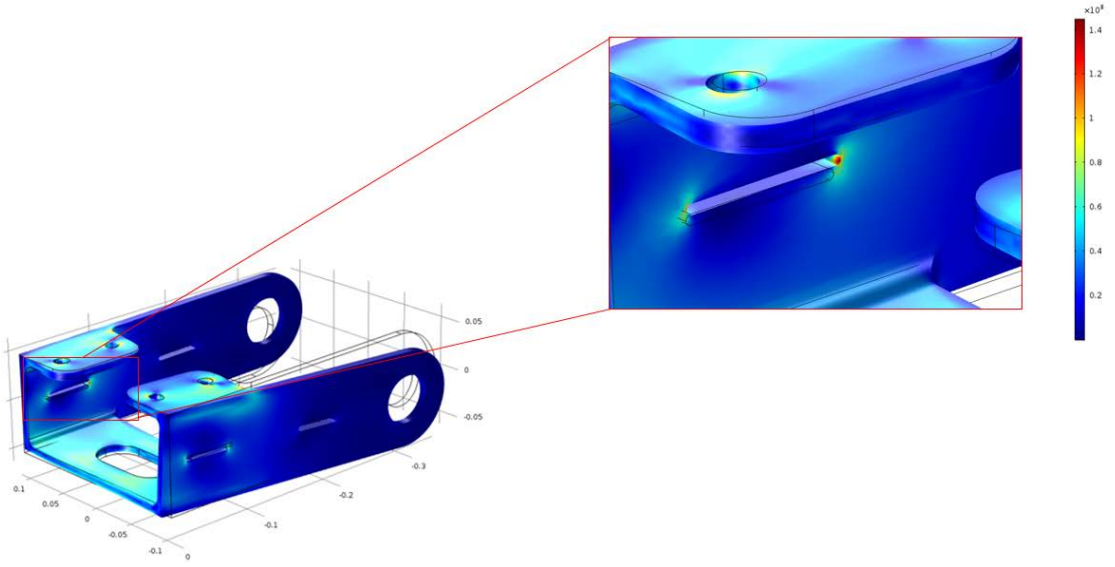

Figure 7: Failure mode C is characterized by an input set in which the parameter defining the length of slot 3 gets large and the parameter describing the height gets small. This creates a stress concentration that induces fatigue failure.

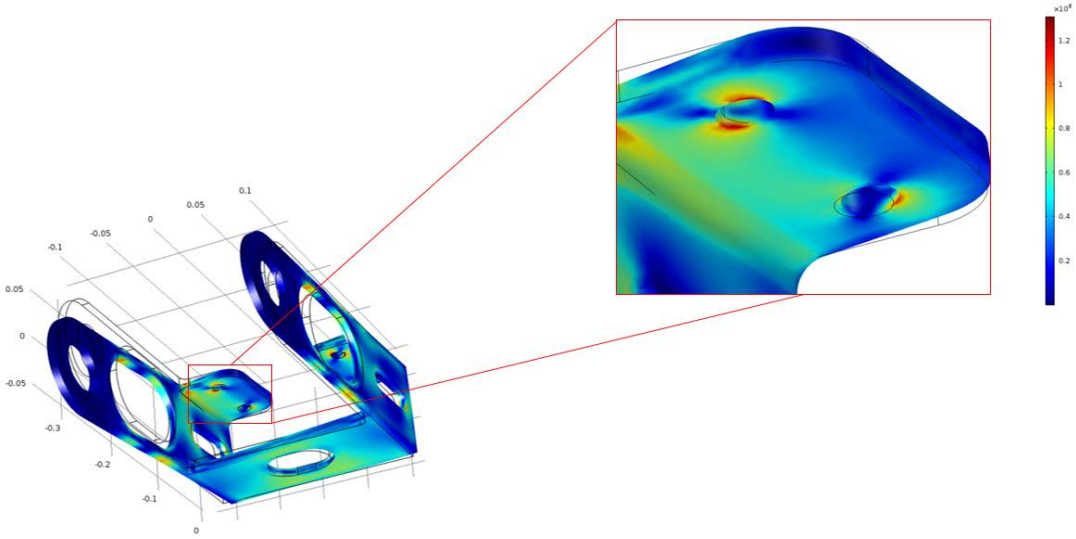

Figure 8: Failure mode D, located at the front bolt hole, is fairly common and seems to occur when the slots get large and twist of the bracket increases.

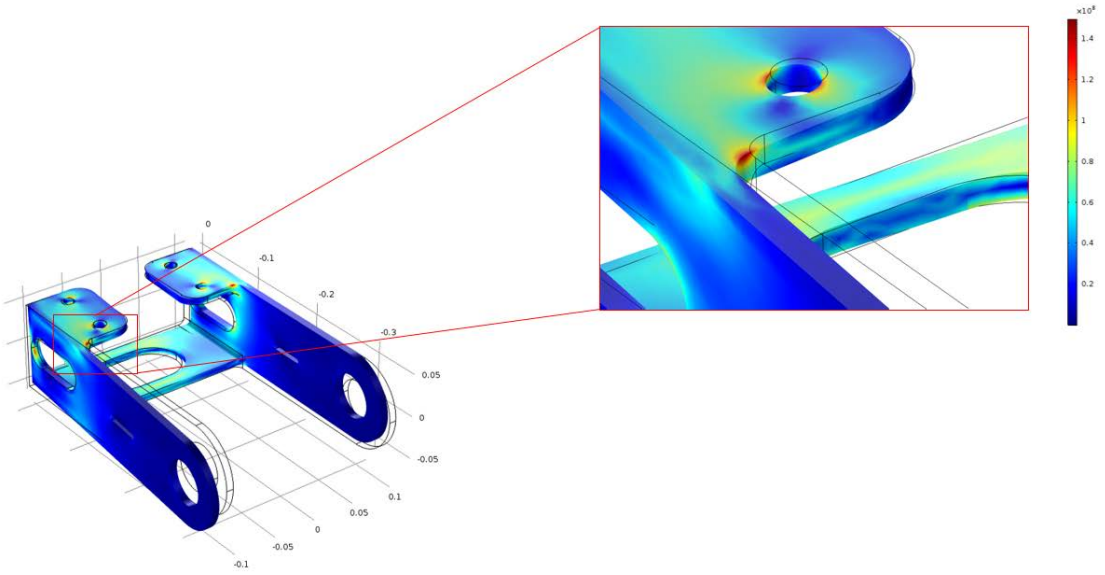

Figure 9: Failure mode E is located at the corner of the flange and is the most common failure mode. It covers almost the entire design space.

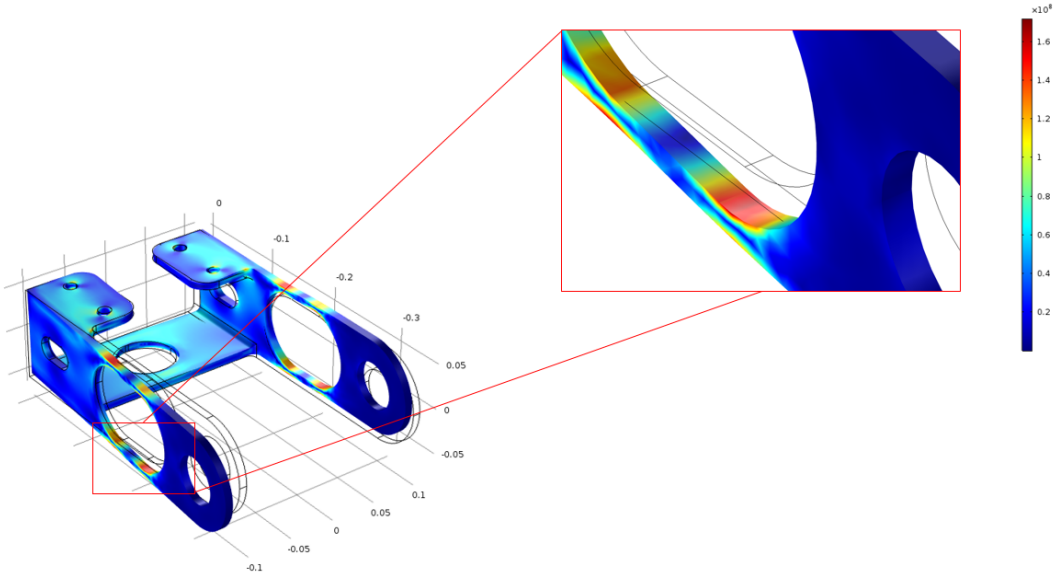

Figure 10: Failure mode F along the edge of slot 1 and tends to occur when slot 1 gets too large and the region between slot 1 and the outer surface of the bracket becomes too thin.

Mixed Input Emulation

Based on the initial results, the problem is more complex than was previously thought. The existence of numerous failure modes renders the multivariate emulator incapable of accurately modeling this problem without significantly more data. Implementation of a Mixed Inputs Classification Emulator offers a way to more effectively use the current data set for further analysis.

SmartUQ's mixed input emulation capabilities are flexible and can handle a wide array of problems where classifying inputs and outputs may be necessary. Here, the Mixed Input – Classification Emulator is used to make predictions not only on the outputs of concern but on the type of failure encountered. For this problem, the emulator will be able to predict the fatigue life, maximum displacement, and mass of each set of inputs while classifying the type of failure expected for that input set.

Figure 11 shows the leave-one-out cross validation results of the Mixed Input Emulator fit to the initial training data. Mass and displacement are well correlated but the fatigue predictions, while greatly improved for most training points (compare to **Figure 4**), still describe some failure modes poorly. **Figure 12** isolates those failure modes, namely A, B, C, and F. It is notable that these failure modes have far fewer points in the training data set than the well described modes D and E. These failure modes lack sufficient training points because they exist in small regions of the design space and the input dimensionality is far too high for the initial DOE to sample these regions properly without many more points being added to the DOE.

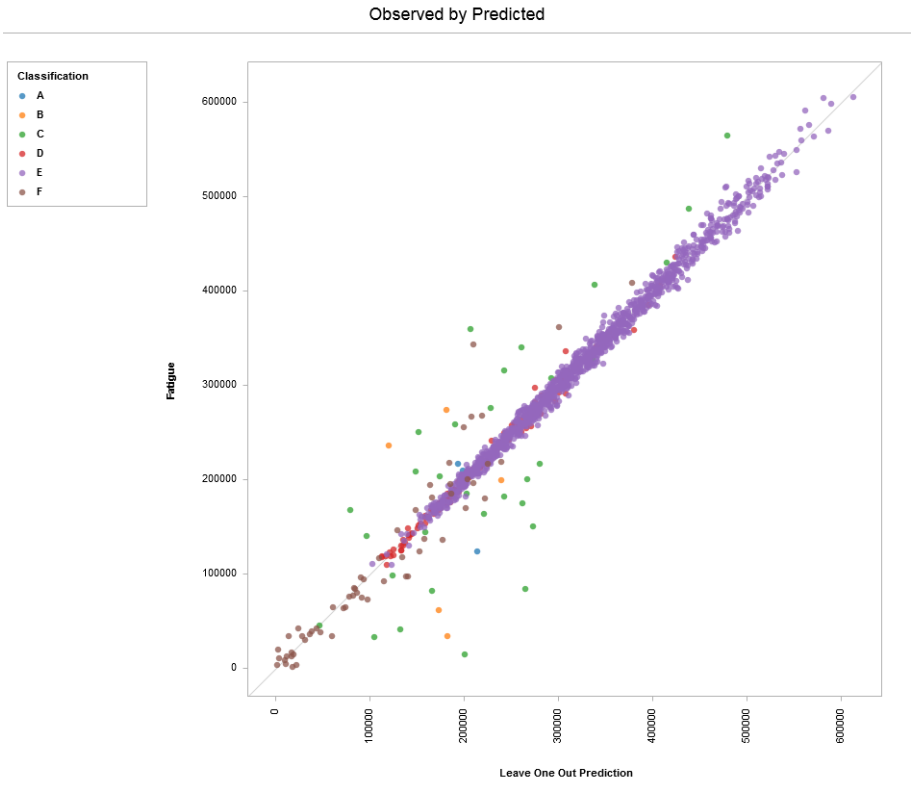

Figure 11: Scatter plot of Leave One Out Prediction vs Fatigue for all of the failure modes.

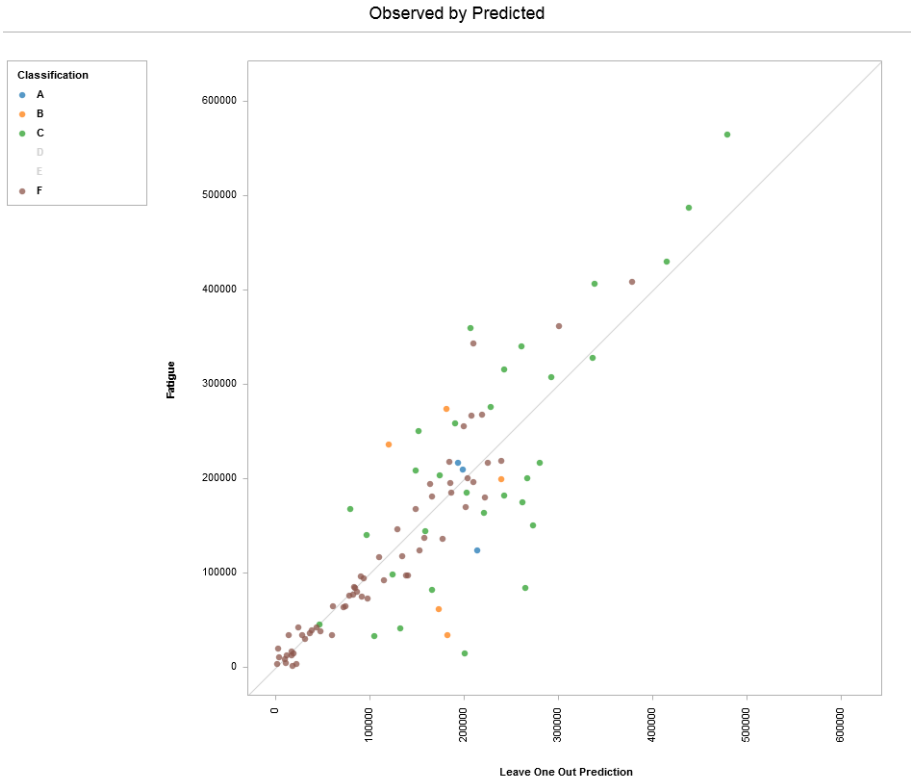

Figure 12: Scatter plot of Leave One Out Prediction vs Fatigue for the poorly characterize failure modes.

Integration of Adaptive Design

There are two paths for improving the correlation of the poorly characterized failure modes. The first would be to run a much larger Sliced DOE and brute force simulations until these regions were well defined. This would be very inefficient: the vast majority of design points for the initial DOE lie within the bounds of failure mode D or E and only a small percent lies within other failure modes. For instance, failure mode A occurs only 3 times out of 1400 trials (0.2%) in the initial DOE. Tens of thousands of simulations would need to be run, with an enormous computational cost, in order to accurately characterize all of the failure modes.

The second path uses the already generated Mixed Input Emulator to examine and isolate the design spaces corresponding to each of the failure modes. Individual emulators can then be created and SmartUQ's advanced Adaptive DOE can be used to intelligently select new design points that target the regions containing the poorly characterized failure modes. By narrowly targeting regions of the design region, this process greatly reduces the number of additional samples required to accurately characterize these failure modes. Using the process summarized below, what could have taken tens of thousands of simulations using a traditional DOE instead required 160 new simulations.

First, the design spaces of each failure mode need to be isolated. The Mixed Inputs visualization tools serve as an excellent method to do this.

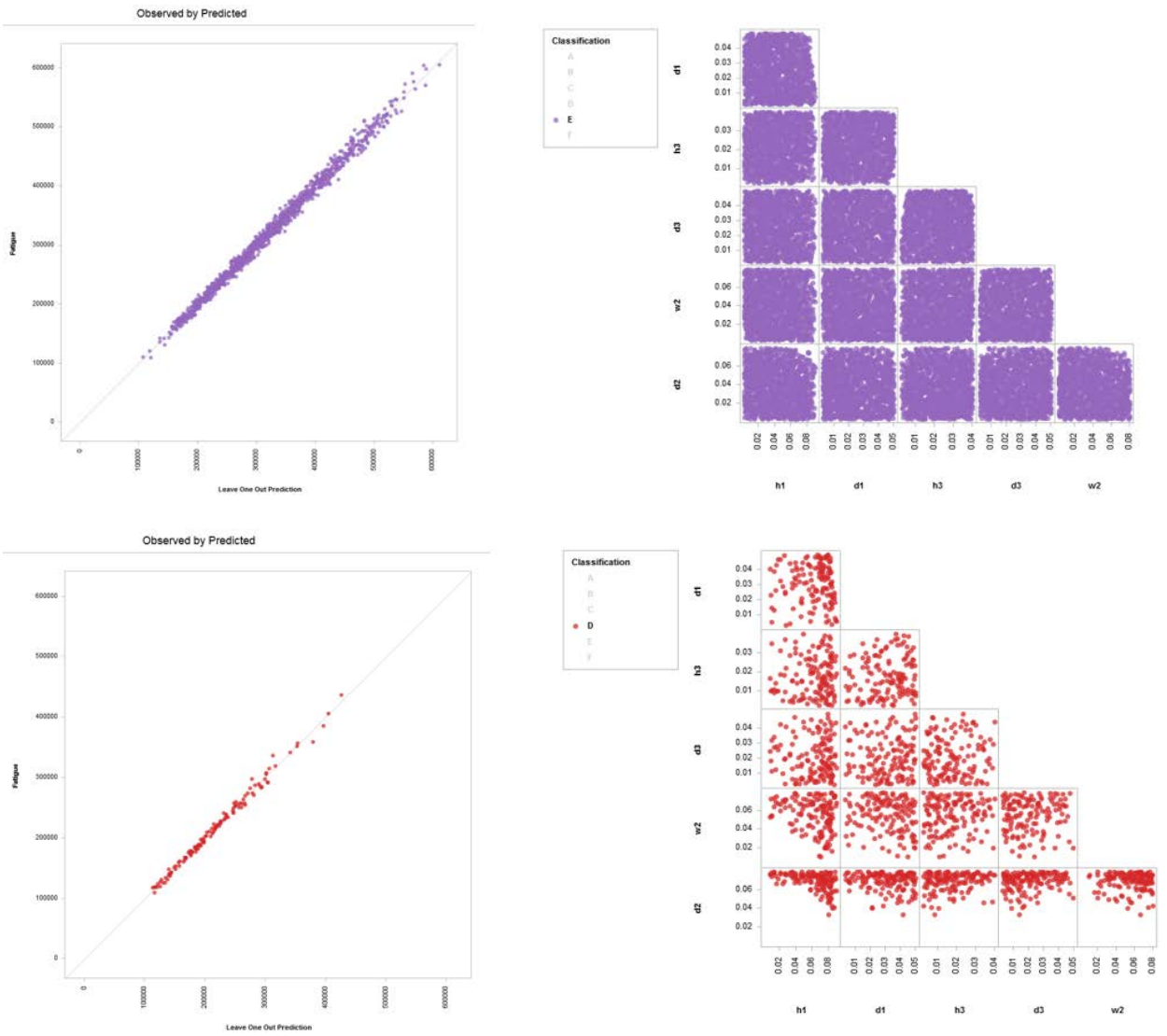

Figure 13: Leave One Out Prediction scatter plot (left) and input design space (right) for failure mode E (top) and failure mode D (bottom).

It is evident from **Figure 13** that failure modes D and E cover large swaths of the design space and are already very well characterized – an Adaptive DOE will not be required for these regions. As **Figure 12** indicates, this is not the case for the other failure modes. The scatter plots in **Figure 14** show the design space occupied by the other failure modes. For clarity, these scatter plots only contain the six inputs corresponding to the geometric design parameters. The full input space is 12-dimensional and the remaining inputs describing uncertainties in the testing conditions and machining tolerances associated with the slots. These additional inputs will be used for further analysis after the emulation process is complete but currently, are not of interest as they have little bearing on the failure mode.

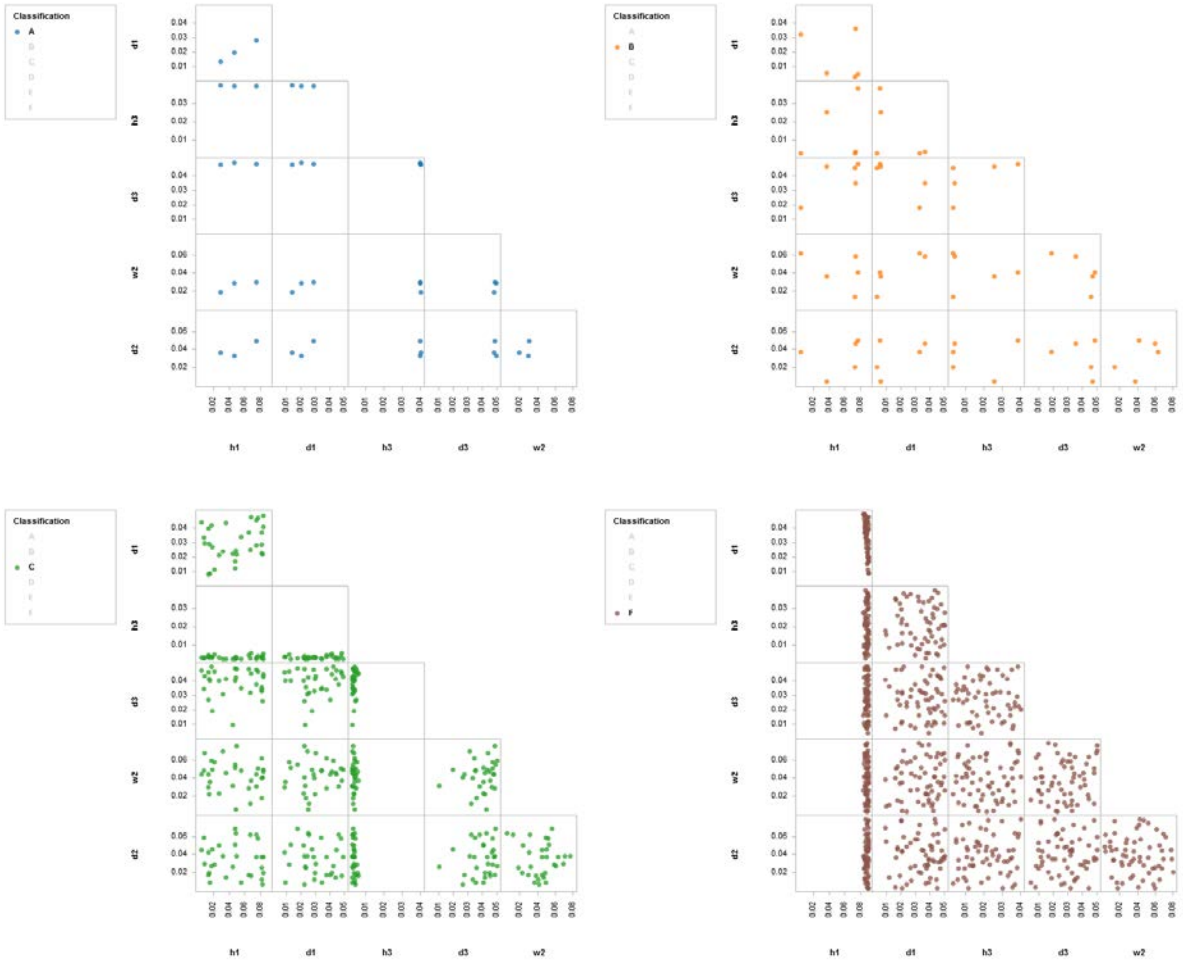

Figure 14: Geometric design input spaces for the poorly characterized failure modes.

An Adaptive DOE was carried out on each of these design spaces. The process will be shown for the design space corresponding to the failure mode with the least initial design points, Failure Mode A, and then the results of the overall adaptive design will be summarized.

The first step in running an adaptive design on this mixed-input system is isolating a failure mode of interest, in this case failure mode A. The data points corresponding to this failure mode are then used to fit a univariate response emulator. **Figure 15** shows the emulator created from these points. Though the design space corresponding to mode A is fairly narrow, this is still a 12-dimensional problem and three points is nowhere near enough to characterize this space. To apply an adaptive design to the emulator, 20 Model-Driven runs and 20 Space-Filling runs are added. Model-Driven Augmented runs use information from the emulator to intelligently place additional input points where they are most needed for the design. The Space-Filling Augmented runs pay attention only to the emulator's current input design space and aim to optimally fill the entire space. For such few initial points, the space filling algorithm would generally be used first before adding on additional, model-driven points, but for illustration both are performed in the same step here.

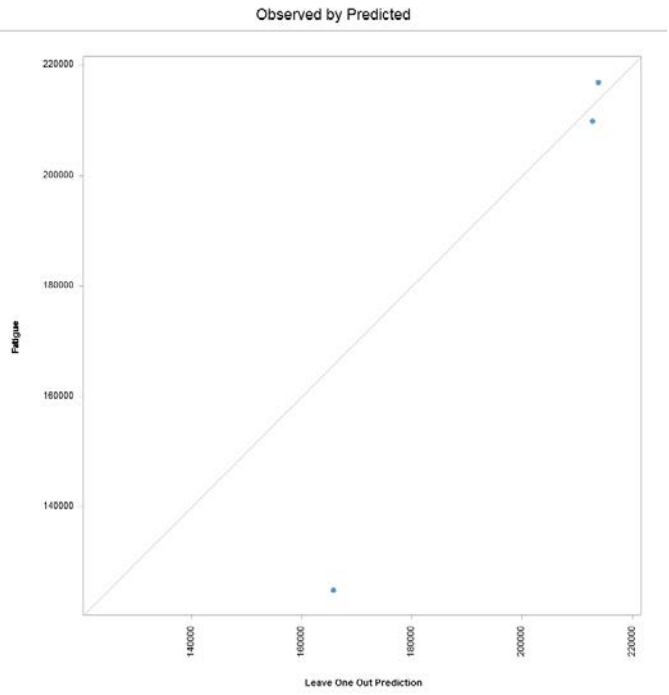

Figure 15: Leave One Out Prediction scatter plot for the failure mode A's design space**.**

Figures 16 and 17 illustrate the Adaptive Design process in terms of generating new input points. First, how they fit in failure mode A's restricted design space, and then how the points fit in the design space globally.

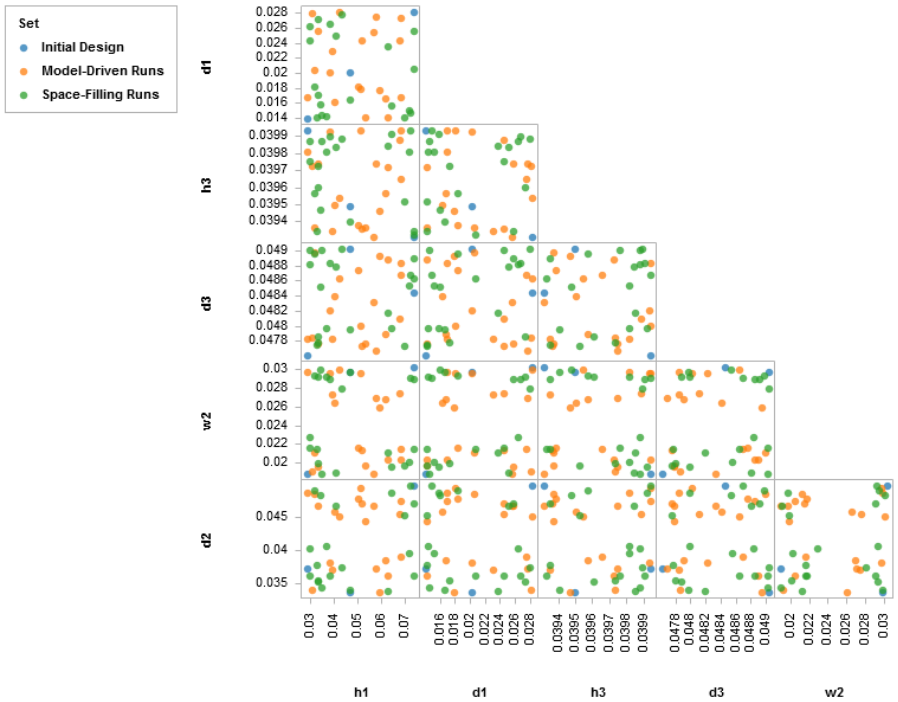

Figure 16: Adaptive design points in failure mode A's individual Design Space

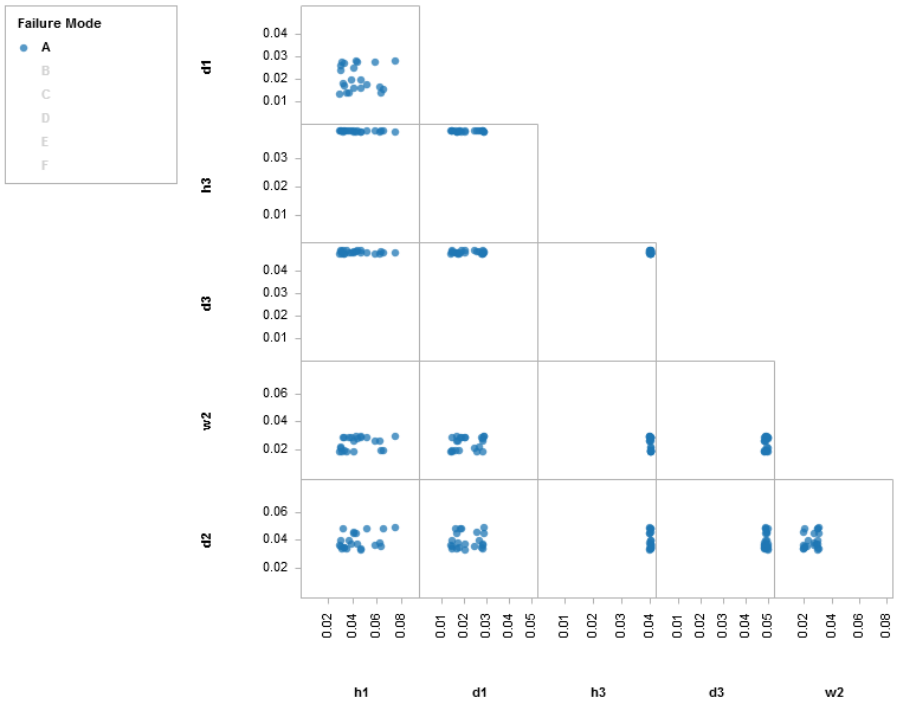

Figure 17: All of failure mode A's design points in the overall design space.

It can be seen clearly from **Figure 17** that the Adaptive DOE algorithm accurately targets points of interest concerning failure mode. These new design points are then run through the simulation in COMSOL to generate a corresponding set of outputs. The new data set is then combined with the original data set and used to make a new Mixed Input Emulator. **Figure 18** shows the improvement from the initial emulator to the emulator after the Adaptive DOE study for failure mode A. The agreement between the training data and the emulator prediction improves significantly.

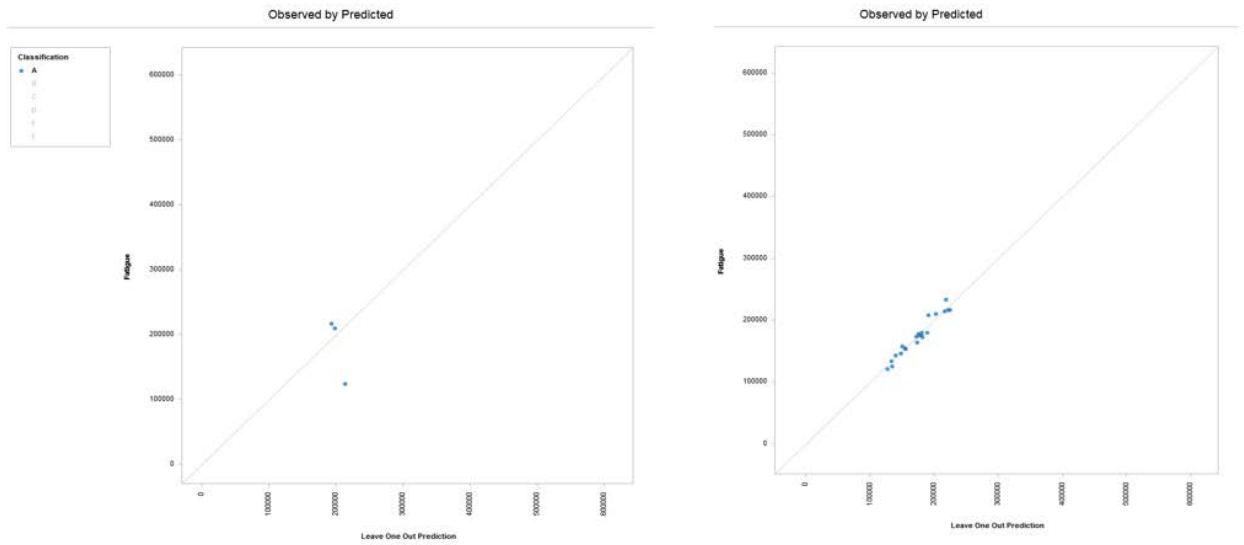

Figure 18: The Leave One Out Prediction for the initial design points (left) and final design points (right) for failure mode A.

This process is carried out for each of the four poorly characterized failure modes. **Figure 19** shows the Leave One Out Prediction scatter plot for the emulator formed after one round of the Adaptive Design. Correlation improves for each of the failure modes, though failure mode C still shows significant error. While it isn't necessary for this example, the Adaptive Design process could be repeated until each failure mode met a certain standard of accuracy (i.e. RMSE of a test group etc.).

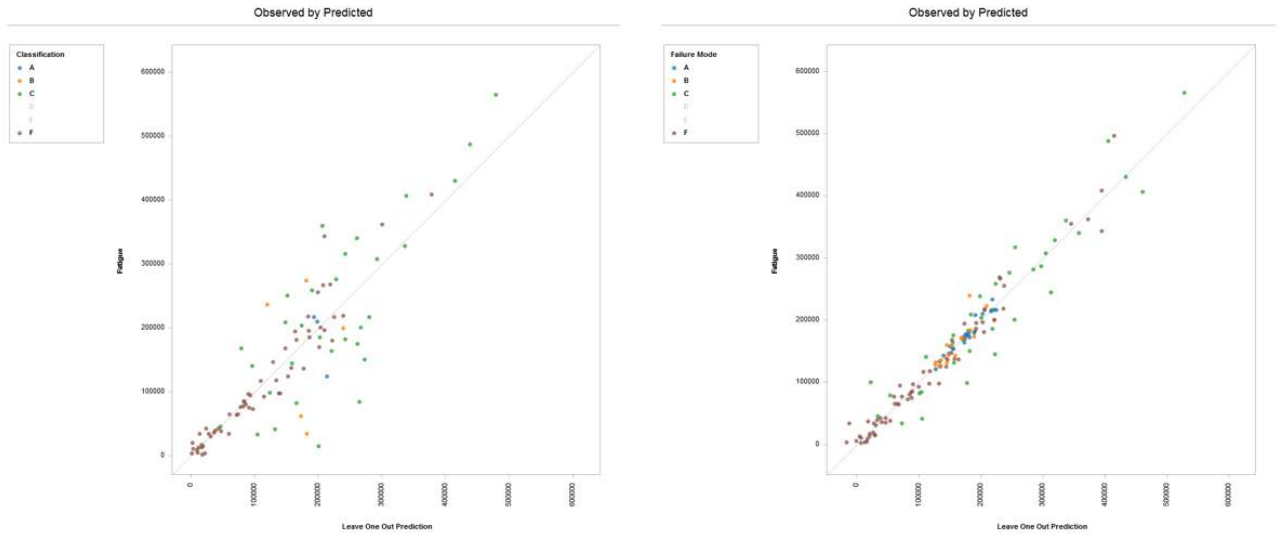

Figure 19: The Leave One Out Prediction for the initial Mixed Input Emulator (left) and the Mixed Input Emulator generated after the adaptive DOE (right).

As **Figure 19** indicates, the correlation between predictions and training data is greatly improved by only increasing the number of simulations by about 10%. One or two more iterations of this approach would yield even more accurate results. To put this in context, the Adaptive Design approach increases the instances of failure mode A by 40 points (from the initial three). To get this many points for failure mode A using a traditional DOE, the number of trials would need to be increased from 1400 to 18,700 – an unnecessary computational burden. The combination of Mixed Inputs Emulation and Adaptive Design greatly increases the efficiency of characterizing these failure modes.

Design Exploration and Analysis

Optimization of Bracket Design

Now, with an emulator properly trained to handle the particular challenges of this problem, optimization can be performed. Since failure modes D and E do not occur at locations on or near the slots, they will be the most robust to uncertainties in the manufacturing of this bracket and are therefore the most stable failure modes. Failure mode D, however, is characterized by a significant twisting in the bracket due to reduced torsional stiffness and will need to be avoided to meet displacement constraints. Therefore, since failure mode E is the most stable and covers the largest area of the design space, it will be isolated and used for optimization. The results of the optimization will then be processed by the Mixed Input Emulator to ensure that the optimal point is indeed characterized by failure mode E.

Failure mode E is isolated from the Mixed Input Emulator and used to generate a multivariate emulator. The cross-validation scatter plot is shown in **Figure 20** below.

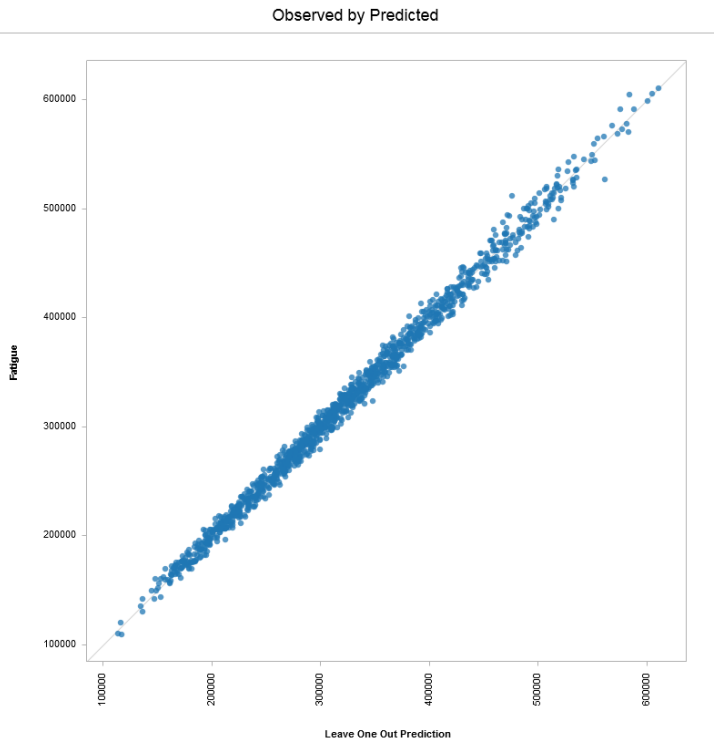

Figure 20: Leave One Out Prediction for the multivariate emulator based on failure mode E.

The fitted emulator was then used to perform a multivariate optimization with the goals summarized in **Table 3**.

Output Parameters	Original Design	Optimization Goals
Mass (kg)	6.03	Minimize
Fatigue (N)	460,000	> 400,000
Displacement (mm)	2.28	< 2.5

Table 3: Summary of optimization goals.

To run the optimization, constraints need to be set to restrict the optimization algorithm from exploring design space inhabited by other failure modes. Inspection of the mixed input emulator makes determination of these bounds easy, as depicted in **Figure 21**. The three most important factors contributing to the alternative failure modes are h1, h3, and d3. **Figure 22** shows the constraints set to the inputs for the optimization. The results of the optimization are summarized in **Table 3** and **Figure 23.**

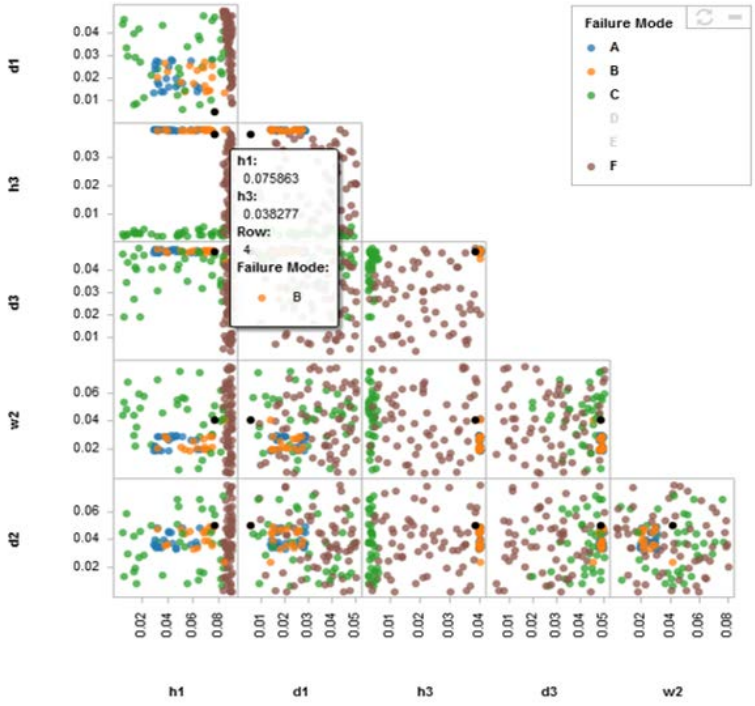

Figure 21: Design space with the failure modes A, B, C, and F isolated.

Factor	Lower Bound	Upper Bound
h1	0.0025273	0.08
d1	0.0025148	0.049985
h3	0.006	0.0375
d3	0.0025148	0.044
w2	0.0025242	0.079976
d2	0.0025727	0.079976
delx1	0	0
dely1	0	0
delx2	0	0
dely2	0	0
delx3	0	0
dely3	0	0
EI	200000000000	200000000000
Sn	1	1

Factor bounds set to restrict optimization from exploring design space of other failure modes.

Uncertainty parameters normalized for optimization. Will come into play for sensitivity analysis, uncertainty quantification, and data calibration.

Figure 22: Factor bounds for multivariate design optimization.

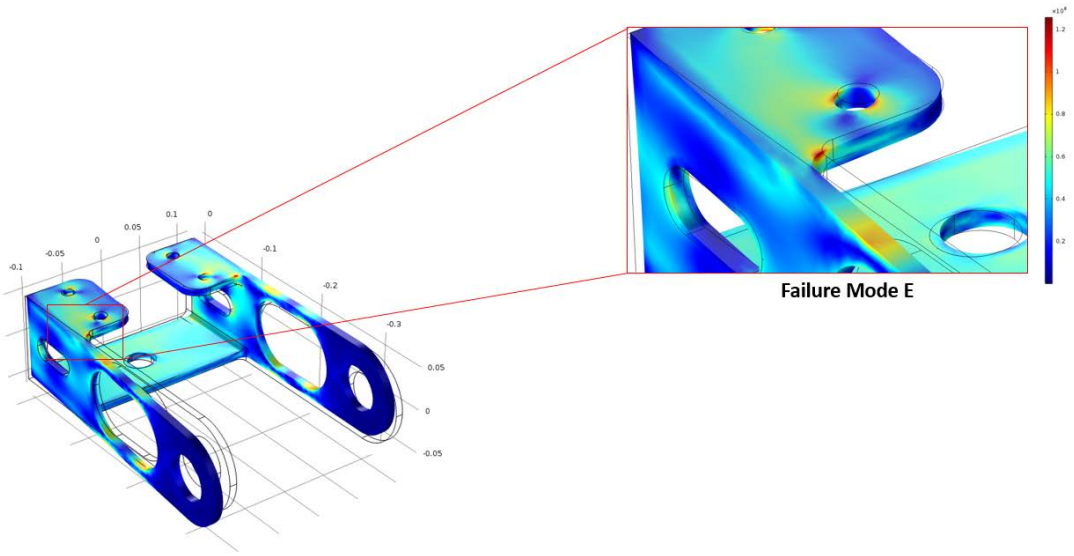

Figure 23: COMSOL validation test of the optimal configuration confirms the location of the desired failure mode. The geometric parameters also produce the failure mode E when run through a prediction in the Mixed Input Emulator.

	Original Design	Optimum Prediction	COMSOL Validation
Displacement (mm)	2.28	2.49	2.53
Mass (kg)	6.03	4.717	4.718

Fatigue (N)	460000	457658	459300

Table 4: Summary of optimization results and COMSOL validation.

Examination of **Table 4** indicates that the displacement constraint is the limiting factor of this optimization. The fatigue life is barely effected by this input configuration whereas the displacement is right at the upper bound set in the optimization constraints. Mass was reduced significantly, by about 1.3 kg, but could clearly be reduced further with a less stringent constraint on the maximum displacement. By using an emulator in an actual design setting, these tradeoffs could be quickly explored by the design engineer.

Sensitivity Analysis

Important information can be gleaned from performing a Sensitivity Analysis (SA) on an emulator. SA quantifies to what extent each input parameter impacts the output parameters for a given range of the input parameters. This is useful in determining which parameters are the most important to concentrate on in a design and which can be set aside in future analysis.

An SA was performed on the geometric parameters for the emulator describing the bracket. **Figure 24** shows the results of this analysis.

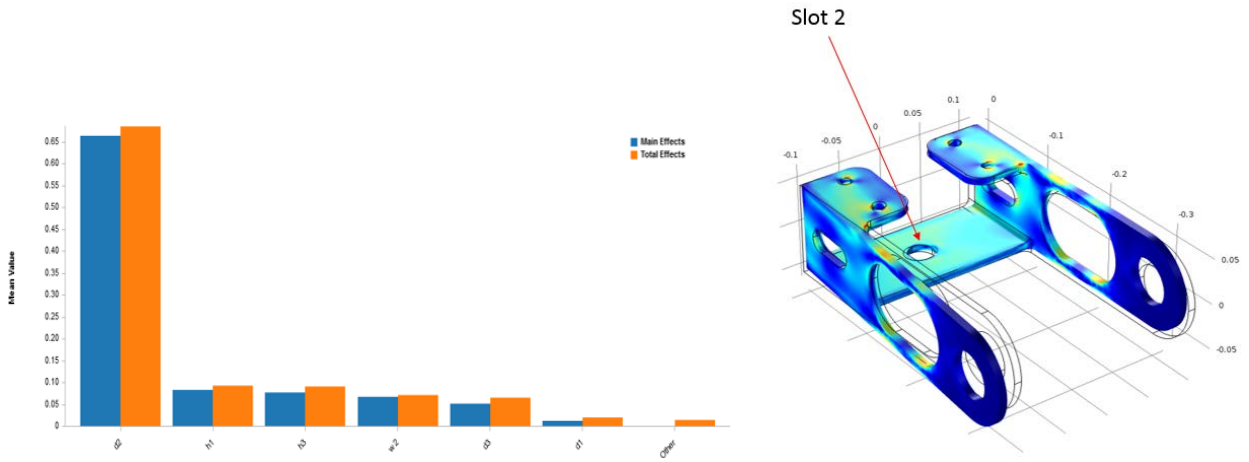

Figure 24: Sensitivity Analysis performed on the bracket's geometric parameters.

The SA performed on the bracket yields an interesting result. The most important parameter affecting fatigue is d2 by a large margin, which describes the length of slot 2, pictured in **Figure 24.** This likely because increasing the size of that slot greatly reduces the torsional stiffness of the bracket, which amplifies the twisting motion. This also explains why the optimization algorithm minimized this parameter. This result indicates that it may be wise to forego cutting a slot in this location altogether.

Uncertainty Propagation

A design's robustness to uncertainty must be considered before being finalized. This data set contains a number of parameters corresponding to the uncertainty in the design due to machining tolerances and

variation in material properties and test conditions. The bounds for the parameter uncertainty are set according to **Table 5.**

	Optimized Parameters	Lower Uncertainty Bound	Upper Uncertainty Bound
h1	0.079564382	0.075586162	0.083542601
d1	0.046938073	0.04459117	0.049284977
h3	0.025169252	0.02391079	0.026427715
d3	0.034232464	0.032520841	0.035944088
w2	0.002782428	0.002643306	0.002921549
d2	0.029803104	0.028312949	0.03129326
delx1	0	-0.0001	0.0001
dely1	0	-0.0001	0.0001
delx2	0	-0.0001	0.0001
dely2	0	-0.0001	0.0001
delx3	0	-0.0001	0.0001
dely3	0	-0.0001	0.0001
El	2E+11	1.90E+11	2.10E+11

Table 5: Upper and lower bounds for the uncertainty parameters.

With these bounds, the Uncertainty Propagation study is run. **Table 6** and **Figures 25** and **26** show the resulting uncertainty distribution for fatigue and maximum displacement respectively.

Output	Mean	Standard Deviation
Displacement	0.002495092945349	0.000045899418735
Stress	125709375.50515938	523728.16195562924
Mass	4.716498865725955	0.0518123603145701
Fatigue	457267.4544350889	9305.31902926268

Table 6: The mean and standard deviation of the outputs for uncertainty propagation.

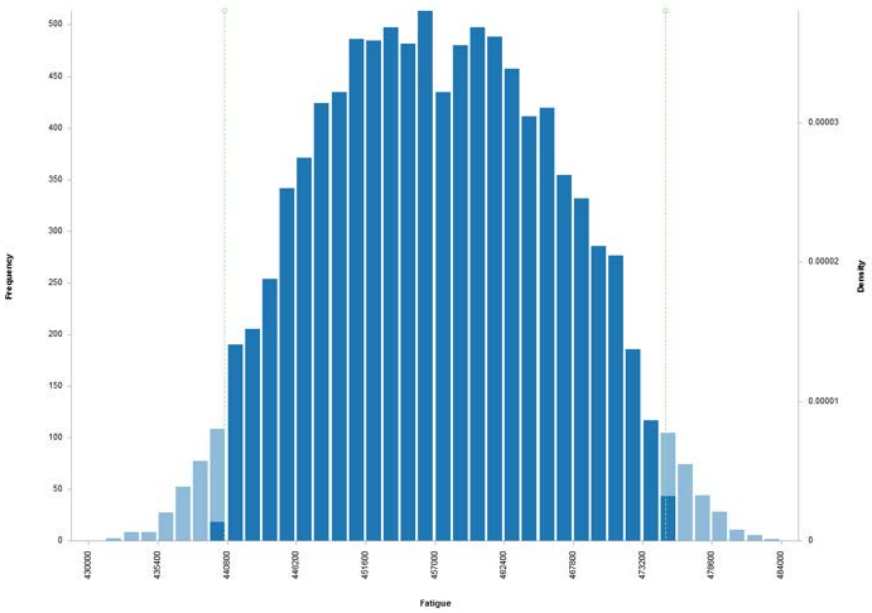

Figure 25: Fatigue distribution of optimal design due to propagated uncertainties in the design.

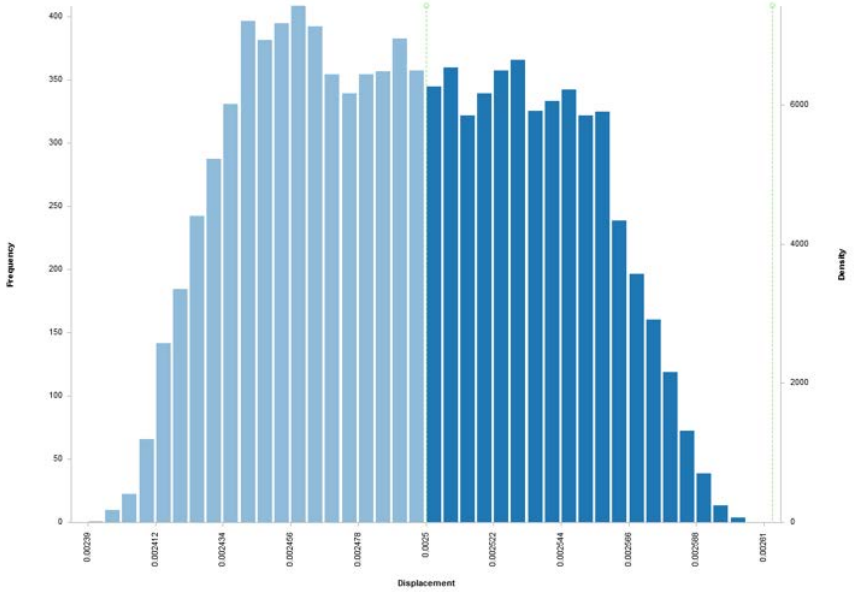

Figure 26: Displacement distribution of optimal design due to propagated uncertainties in the design.

Figure 25 indicates that the design is fairly robust to fatigue and that the current design is certain to meet the requirements set for fatigue. This isn't quite the case for displacement. As compared to fatigue, the displacement parameter is not as robust to uncertainties. As **Figure 26** indicates, there is a 46% chance that the current design will not meet the design goals. This is caused by the optimization result taking the

displacement right to the edge of its design constraint. If this result is unacceptable, the design engineer can use this information to reset the constraints of the optimization and then rerun it. If this margin of error is inconsequential, for instance if a large factor of safety was already implemented, then the engineer could go forward with this design.

Statistical Calibration

Statistical calibration is a growing area of study in the aerospace and automotive industries. The ability to calibrate various simulation parameters to physical experiments is a powerful tool. For the bracket case study, a number of uncertainties in test conditions and material properties could cause disparities between results garnered in the lab and those developed computationally. For simplicity, the wide variety of possible parameters that could contribute to these uncertainties will be reduced to two parameters: El and Sn. El represents variation in the material properties due to manufacturing uncertainty, the modulus of elasticity in this case. Sn represents a possible disparity between the conditions the S-n curve used to determine fatigue from the simulation stress output and the S-n curve corresponding to the conditions the physical tests are being run under. It's highly unlikely that physical tests designed to mimic a particular part's expected use conditions will match those corresponding to a standard S-n curve used for reference in a simulation. This will create a disparity between the fatigue results of the simulation and physical tests that the Sn parameter aims to correct.

SmartUQ uses advanced DOE technology that allows generating DOEs for simulations and physical testing such that performance under calibration is optimized. The tool allows the user to either construct these simulations and experimental DOEs simultaneously or to subsample the experimental DOE from a simulation DOE that's already been implemented. Both of these methods are reviewed below.

Simultaneous Construction is the first DOE offered by SmartUQ for the purpose of Statistical Calibration. This method uses fractional factorial design selection to pick the optimal set of experimental points. A DOE for simulation incorporates these points and then optimally constructs a DOE around them, corresponding to the number of extra points selected for the simulation. **Figures 27** and **28** show the resulting DOEs generated with this setup.

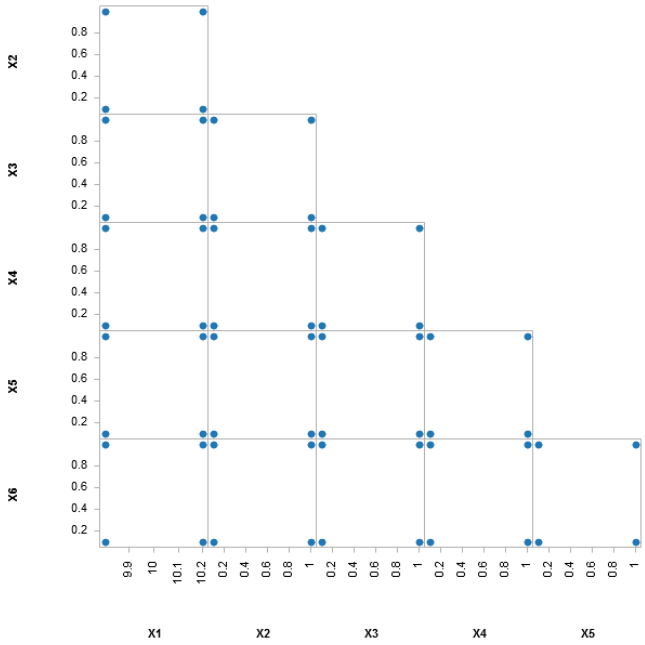

Figure 27: Experimental DOE with 16 points placed using a fractional factorial design.

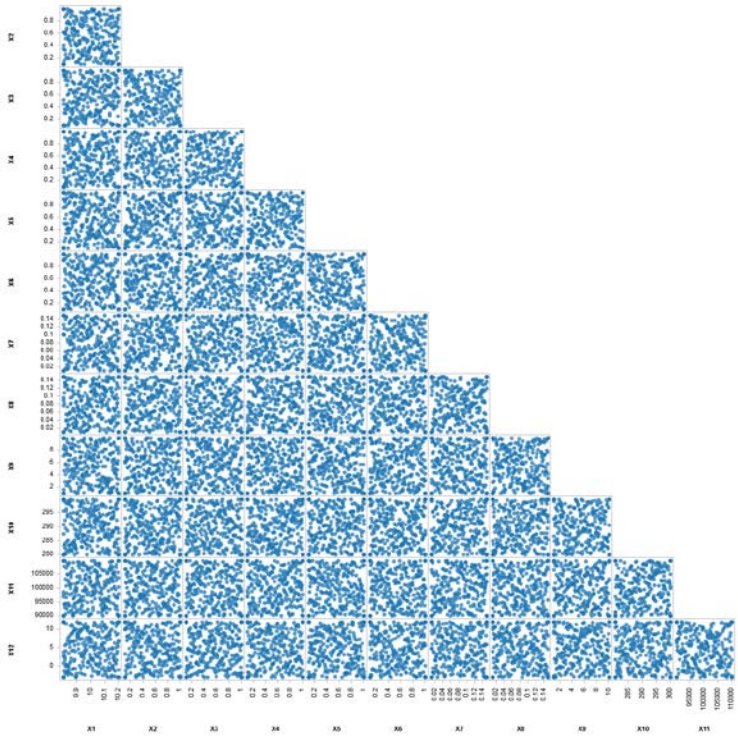

Figure 28: Simulation DOE with an additional 250 points placed by first incorporation the Experimental DOE points and then constructing a DOE with the additional points around them.

As **Figure 27** and **28** indicate, the experimental DOE will tend to have far fewer points and will have fewer dimensions than the simulation DOE. The extra dimensions in the simulation DOE will either be constrained to particular values of interest or calibrated to fit the experimental data.

The second method for constructing a DOE for Calibration is taking the DOE of a simulation design and sub-selecting a desired number of points from the appropriate dimensions. While not as optimal as Simultaneous Construction, this method is an effective alternative if a data set already exists for a particular simulation. This is the method that will be used to calibrate the bracket simulations to the experimental data generated for that example. Here 20 points will be sub-selected from the original simulation DOE to perform the experimental trials. The "physical tests" performed for this study were simulations run under alternate conditions, with significant, random noise added to the outputs, so as to assess the performance of the calibration study against the known result. **Figure 29** shows the final experimental DOE.

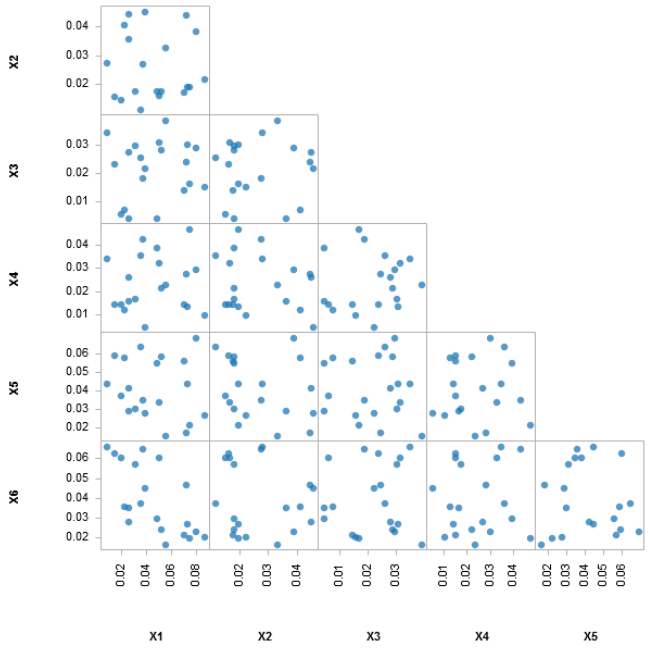

Figure 29: Experimental DOE generated using the above setup.

After the Experimental DOE was created, the "physical data" could be generated. Actual applications of this process would involve running a fatigue test on the different part designs specified by the DOE under the relevant conditions and then using the data generated to calibrate the simulations. As mentioned previously, this data was generated using the same simulation under purposefully altered conditions so as to provide both bias and noise to the experimental data. This makes it possible to assess the effectiveness of the calibration tool since the true result and the magnitude of the modifications are known.

For the calibrated emulator, the simulation and physical data share variation in the geometric parameters but only the simulation data includes parameters associated with the material and test condition

uncertainties, Sn and El. These two parameters will be calibrated such that the simulation data matches the trends seen in the physical data.

Upon generating a calibrated emulator, SmartUQ provides a number of discrepancy distribution and function plots to assess the quality of the calibration. **Figure 30** plots the distribution of the discrepancy between the calibrated emulator and physical data for the fatigue. Because the discrepancy is small, relative to the magnitude of the average fatigue life, and distributed randomly about the x-axis at zero, the calibrated emulator is likely a strong model of the physical data. **Figure 31** shows the discrepancy function Multiview for all of the output parameters. Again, since the distributions tend to be small and randomly distributed, the final emulator is well correlated.

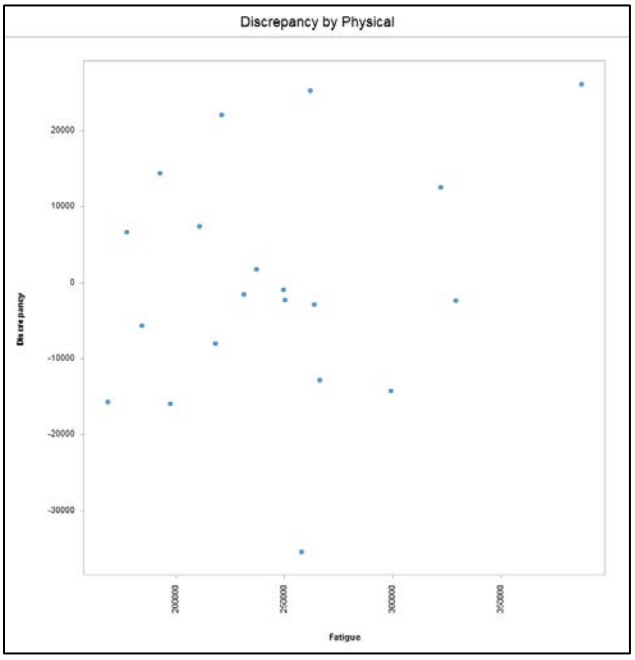

Figure 30: Discrepancy scatter plot for the fatigue life output for the calibrated emulator.

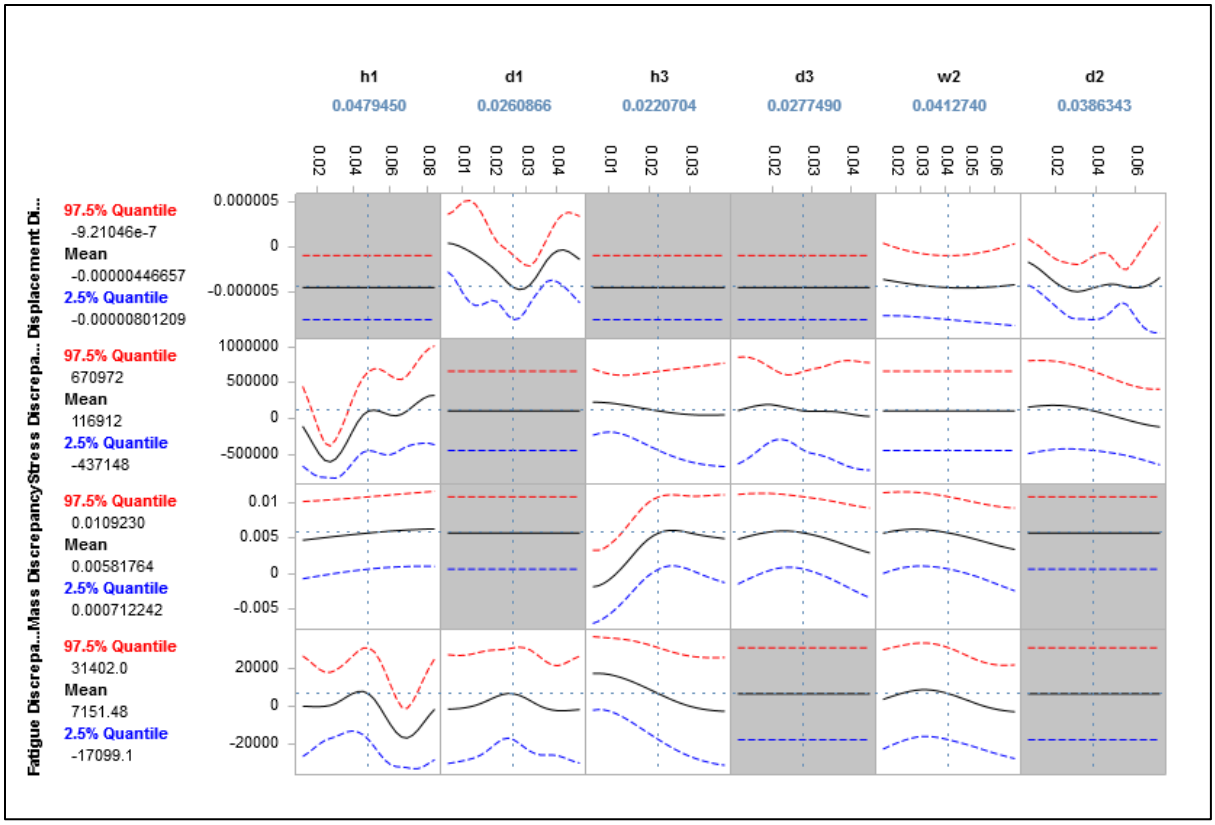

Figure 31: Discrepancy distribution multi-view for all of the output parameters vs the geometric inputs.

Once the process is completed, the calibrated emulator outputs the calibration parameters it arrived at during the calibration process. In this case, the parameters El and Sn were calibrated to values of 1.99e8 and .811, respectively. The physical tests in this case were mimicked by simulations with specifically offset values for these parameters, 2.00e8 and .800, respectively, along with a significant amount of noise to replicate real physical tests. These results, as well as **Figure 32** below, indicate how close the calibrated parameters can get to the true result despite noise, and a significant bias, in the data.

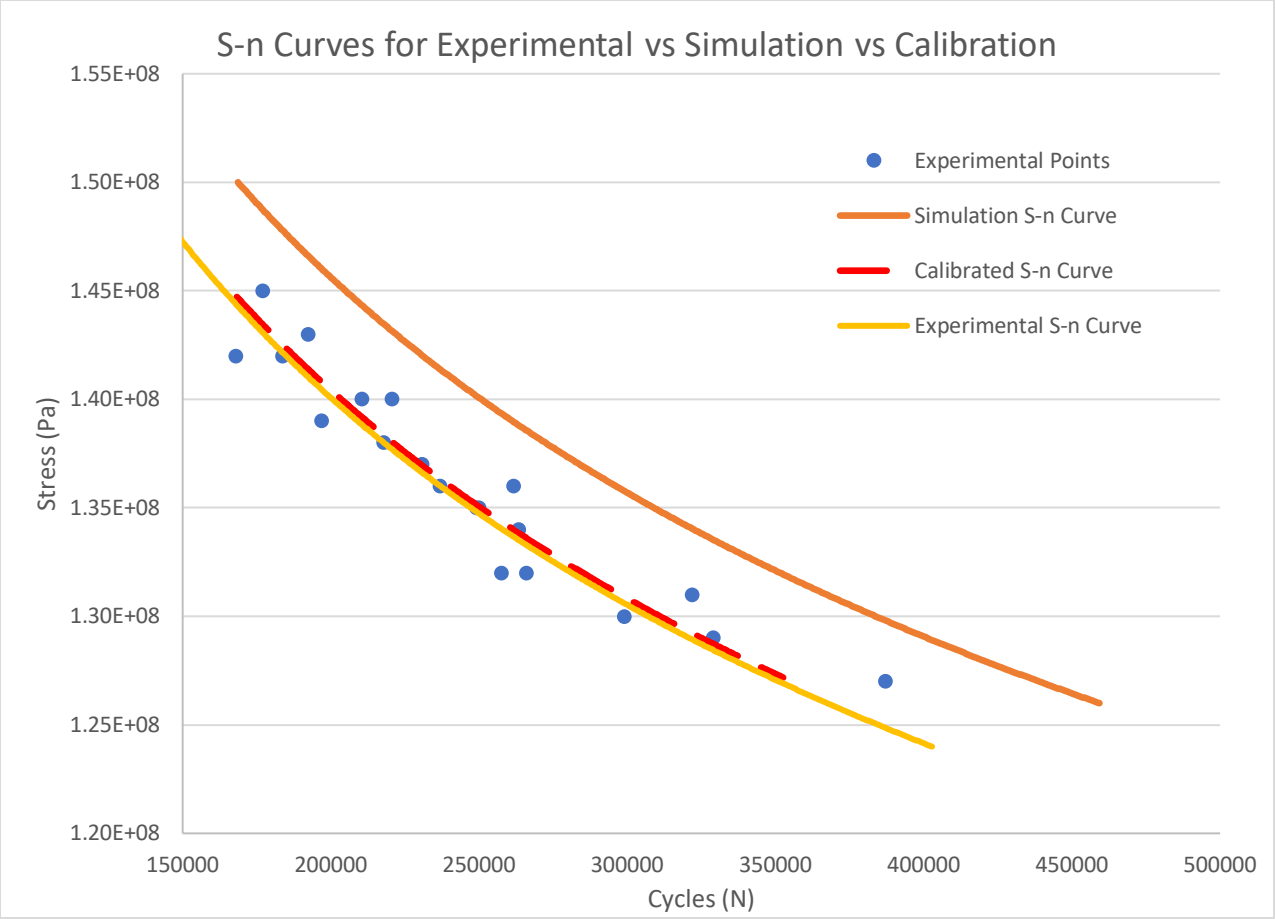

Figure 32: Summary of calibration study. The experimental data (blue and yellow) has significant bias and noise compared to the original simulation and emulator (orange). The calibrated emulator (red) is able to capture the bias in the data, and therefore, the "true" result, while avoiding adverse effects of noise.

Once the calibrated emulator is generated, optimization, sensitivity analysis, and uncertainty propagation can all be performed to analyze the design of the bracket under the new conditions. This process would look similar to the previous section.

Conclusion

A broad range of analytical tools were used to take a bracket design from an initial configuration to a well described, optimized design. This report covered SmartUQ's capabilities in continuous multivariate emulation, discontinuous mixed input emulation, prediction, sensitivity analysis, optimization, and uncertainty propagation. This example also briefly highlighted the powerful calibration tool used by SmartUQ to correct simulations to physical test data. While touching on a few analytical tools, this paper only scratches the surface of the depth to which SmartUQ can be used to make design decisions and garner new understandings of a design's performance.